Effects of Chlorpromazine and Trinitrophenol on the Membrane Motor of Outer Hair Cells

Jie Fang and K. H. Iwasa
Section on Biophysics, Laboratory of Cellular Biology, National Institute on Deafness and Other Communication Disorders, National Institutes of Health, Bethesda, Maryland

ABSTRACT The motile activity of outer hair cells' cell body is associated with large nonlinear capacitance due to a membrane motor that couples electric displacement with changes in the membrane area, analogous to piezoelectricity. This motor is based on prestin, a member of the SLC26 family of anion transporters and utilizes the electric energy available at the plasma membrane associated with the sensory function of these cells. To understand detailed mechanism of this motile activity, we examined the effect of amphipathic ions, cationic chlorpromazine and anionic trinitrophenol, which are thought to change the curvature of the membrane in opposite directions. We found that both chemicals reduced cell length at the holding potential of −75 mV and induced positive shifts in the cells' voltage dependence. The shift observed was ~10 mV for 500 μM trinitrophenol and 20 mV for 100 μM cationic chlorpromazine. Length reduction at the holding potential and voltage shifts of the motile activity were well correlated. The voltage shifts of nonlinear capacitance were not diminished by eliminating the cells' turgor pressure or by digesting the cortical cytoskeleton. These observations suggest that the membrane motor undergoes conformational transitions that involve changes not only in membrane area but also in bending stiffness.

INTRODUCTION

The cell body of outer hair cells (OHCs) has a voltage-dependent motility, which is also known as electromotility (1–3). It is critical for ear function, as illustrated by the hearing loss of mice without normal prestin (4), a protein essential for electromotility (5).

Hyperpolarization induces the cylindrical cell's elongation and depolarization induces shortening. The amplitude is 4–5% of the total length (3). These mechanical changes are associated with charge transfer across the membrane (6), which gives rise to nonlinear membrane capacitance (NLC) with bell-shaped voltage dependence (7,8). Mechanical changes and electric changes are coupled, satisfying the reciprocal relationship (9).

These observations can be successfully described by membrane motor models (or area-motor models), which assume that electromotility is based on a membrane motor that undergoes conformational changes that couple changes in the membrane area with transfer of charge across the membrane (8,10–13). However, it is not certain whether such an area-motor is really a molecular entity that consists of membrane proteins or merely a phenomenological model that conveniently describes experimental observations so far reported. Alternative models include curvature-motor models, which assume that changes in membrane curvature are the source of the motile activity (14–16).

Here we compare the effects of cationic amphipath chlorpromazine (CPZ) and anionic trinitrophenol (TNP), which are thought to bend the plasma membrane in opposite directions (17,18), to obtain insights into molecular events that underlie electromotility. Specifically, we monitor the membrane capacitance and the amplitude of mechanical cell displacement in the whole-cell recording configuration and examine how our observations can be explained.

MATERIALS AND METHODS

Cell preparation

The method for preparing isolated outer hair cells has been described earlier (9). Briefly, bullas were obtained from guinea pigs (in accordance with the protocol 1061-02 NINDS/NIDCD). The organ of Corti was dissociated from opened cochleas by teasing with a fine needle under a dissection microscope. Dispase (Worthington Biochemical, Lakewood, NJ) treatment (1 mg/ml for 10–20 min at 21°C) was used before mechanical isolation. The strips of organ of Corti thus obtained were triturated three times gently with a plastic pipette and placed in a chamber mounted on an inverted microscope. Isolated outer hair cells with the normal shape were chosen for experiments from the cell length ranged between 40 and 75 μm.

Media and extracellular perfusion

The internal solution consisted of 140 mM CsCl, 2 mM $CaCl_2$, 5 mM EGTA, and 10 mM K-HEPES. The external solution contained 140 mM NaCl, 5 mM CsCl, 2 mM $MgCl_2$, 1 mM $CaCl_2$, 2 mM $CoCl_2$, 10 mM Na-HEPES, and ~10 mM glucose, which was used to adjust the osmolarity to 300 mOsm/kg. The pH is adjusted to 7.4. These channel blocking media facilitated capacitance measurements.

Chlorpromazine (CPZ), trinitrophenol (TNP), procaine, and dipyridamole were purchased from Sigma (St. Louis, MO). Each of these chemicals was dissolved in the external medium and put in a perfusion pipette. Perfusion was controlled by a solenoid valve and a pressure reservoir.

Membrane capacitance measurement

Experiments were performed on isolated outer hair cells in the whole-cell recording configuration. The membrane capacitance was determined by

Submitted November 9, 2006, and accepted for publication April 27, 2007.

Address reprint requests to K. H. Iwasa, Tel.: 301-496-3987; E-mail: iwasa@nih.gov.

Editor: Toshinori Hoshi.

0006-3495/07/09/1809/09 $2.00

doi: 10.1529/biophysj.106.100834

capacitive currents elicited by voltage jumps. The voltage dependence of the capacitance was usually determined with a pair of ascending (10 mV steps from −135 mV to +35 mV) and descending (−10 mV steps from +35 mV to −135 mV) staircase voltage waveforms. An alternative voltage waveform ascended from −140 mV to +120 mV in 10 mV steps. The holding potential was −75 mV. The sampling interval of the data acquisition was 10 μs. The pipette resistance was between 2.5 and 4.5 MΩ when filled with the intracellular medium. In the whole-cell configuration, the access resistance R_a was between 5 and 8 MΩ. The membrane resistance R_m was somewhat dependent on the membrane potential and was between 200 and 800 MΩ. The voltage dependence of the membrane capacitance C_m obtained was compensated for the voltage drop due to the access resistance. A patch amplifier (Axopatch 200B, Axon Instruments, Union City, CA) was used for whole-cell voltage-clamp experiments. A train of voltage pulses was generated with an ITC-16 interface (Instrutech, Fort Washington, NY) by using the IGOR program (WaveMetrics, Lake Oswego, OR) with a software module created by R. J. Bookman's laboratory at the University of Miami (http://chroma.med.miami.edu). To concisely describe the bell-shaped voltage dependence of the capacitance we fit our data with a function,

$$C_m(V) = C_{lin} + 4C_{max}\frac{B(V)}{(1+B(V))^2}, \quad (1)$$

with

$$B(V) = \exp[q(V - V_{1/2})/k_BT]. \quad (2)$$

This function has a peak value $C_{max} + C_{lin}$ at $V = V_{1/2}$. The sharpness of the peak is determined by charge q. The quantities k_B and T are, respectively, Boltzmann's constant and the temperature. Equation 1 is consistent with a two-state model in which transition between its two states is accompanied by transfer of charge q across the membrane.

Intracellular digestion

After establishing the whole-cell recording configuration, some cells were injected with the intracellular medium containing 0.1 mg/ml trypsin I (Sigma) from the recording pipette until these cells are fully inflated. After full inflation, small negative pressure was briefly applied to remove turgor pressure. These cells maintained spherical shape after positive pressure to the pipette was removed. As described in a previous report (19), this treatment did not change the nonlinear capacitance characteristic of outer hair cells.

Cell displacement

Images of the cells during the whole-cell voltage clamp experiments were captured and stored in a DVD recorder (model RDR-GX7, Sony, Tokyo, Japan). These images were digitized off-line with an image grabber card (Scion, Frederick, MD) using a computer program (NIH Image, W. Rasband, NIMH, Bethesda, MD). The resolution was 4.04 pixels per μm. Length changes of the cells were determined with a previously developed macro (20). The data obtained were fit with a Boltzmann function,

$$\frac{L(V) - L_{min}}{L_0} = \frac{\Delta L_{max}}{L_0}\frac{B(V)}{1+B(V)}, \quad (3)$$

where $L(V)$ is the cell length at membrane potential V, L_0 the length of the cell at the holding potential, L_{min} the membrane potential independent component of cell length, and ΔL_{max} is the maximum voltage-dependent length change. The function $B(V)$ is defined by Eq. 2 above.

RESULTS

The effects of the amphipathic ions on the voltage-dependent motor of outer hair cells were observed by monitoring the membrane capacitance and axial displacements of the cell. Initially, no attempt was made in changing the turgor pressure of the cell after establishing the whole-cell recording mode.

Nonlinear capacitance and voltage-driven cell displacement

Trinitrophenol (TNP), which is anionic and a crenator of erythrocytes, reversibly shifted the voltage dependence of the motor, monitored by the membrane capacitance, in the positive direction (Fig. 1 *A*). The time constant (mean ± SD) was (6.3 ± 1.5) s (Fig. 1 *C*) at 500 μM concentration (throughout this article, mean values are always accompanied by mean ± SD). The apparent dissociation constant was (68 ± 19) μM and saturated shift was (11.6 ± 0.9) mV (Fig. 1 *D*).

CPZ, which is cationic and a cup-former of erythrocytes, shifted the voltage dependence of the motor, monitored by the membrane capacitance, also in the positive direction (Fig. 2). This shift was also reversible. The time constant was (4.3 ± 1.1) s. The shift was up to (20.3 ± 1.2) mV. The apparent dissociation constant was (16.1 ± 3.7) μM, which was lower than the concentration for micelle formation (21,22).

These effects of TNP and CPZ in shifting the voltage dependence without changing the voltage sensitivity, q, were similar to those of procaine, a cationic amphipath and a cup-former for erythrocytes similar to CPZ, and dipyridamole, a crenator similar to TNP (Table 1).

The effects of these amphipathic ions were not observed in the voltage-independent component C_{lin}.

Cell length at the holding potential

The video record of the cells monitored during the experiment showed that the cell length reduced at the holding potential of −75 mV by perfusion.

Length reduction at the holding potential of −75 mV and the positive shifts in the voltage dependence were correlated (Fig. 3) although the slope for CPZ and TNP differed. The ranges of concentrations were up to 500 μM for TNP and up to 100 μM for CPZ.

A similar reduction of cell length at the holding potential was induced by procaine and dipyridamole. These changes were also accompanied by positive shifts in the voltage dependence (Table 1).

Reduced cell length during perfusion could be the result of increased internal pressure because the cylindrical geometry of the cell requires that the tension in the circumferential direction is larger than the one in the axial direction (23). Such a change could be expected by hyposmotic perfusion. However, that was not the case because the perfusion with the external medium without CPZ or TNP did not change the cell length.

A possible mechanism for increased internal pressure under voltage clamp could be membrane currents. However, membrane currents were small in our experimental conditions because we used channel-blocking media (see Methods

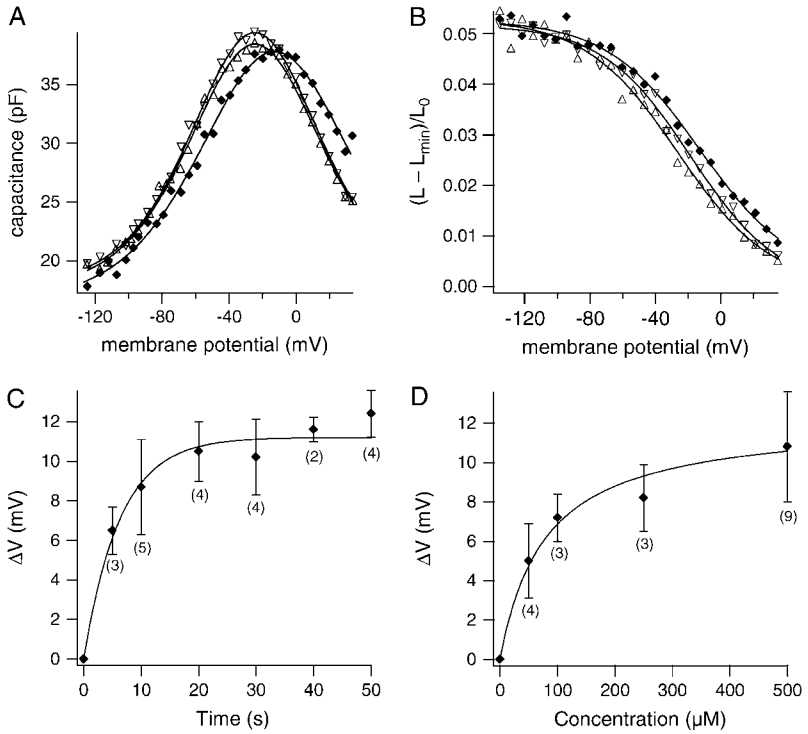

FIGURE 1 Effect of TNP on voltage-dependent capacitance. (*A*) The membrane capacitance plotted against the membrane potential. Control (△), 500 μM TNP (♦), and washout (▽). Parameter values for the fit. Control, q = (0.97 ± 0.02) e, C_{lin} = (17.3 ± 0.04) pF, and $V_{1/2}$ = (− 24.6 ± 0.4) mV. 500 μM TNP, q = (0.86 ± 0.03) e, C_{lin} = (16.3 ± 0.1) pF, and $V_{1/2}$ = (− 12.9 ± 0.7) mV. Washout, q = (0.99 ± 0.02) e, C_{lin} = (17.7 ± 0.4) pF, and $V_{1/2}$ = (− 24.7 ± 0.3) mV. (*B*) Length changes of the cell recorded during the capacitance measurement shown in panel *A*. Control (△), 500 μM TNP (♦), and washout (▽). Parameter values for the fit. Control, q = (0.91 ± 0.11) e, $V_{1/2}$ = (−26.2 ± 3.8) mV, and $\Delta L_{max}/L_0$ = (0.053 ± 0.004). 500 μM TNP, q = (0.91 ± 0.10) e, $V_{1/2}$ = (−12.8 ± 4.7) mV, and $\Delta L_{max}/L_0$ = (0.051 ± 0.004). Washout, q = (0.96 ± 0.08) e, $V_{1/2}$ = (−18.5 ± 3.1) mV, and $\Delta L_{max}/L_0$ = (0.052 ± 0.003). (*C*) Time course of voltage shift with 500 μM TNP. The time constant is (6.3 ± 1.5) s. The saturating shift is (11.2 ± 0.6) mV. (*D*) Dose response. The curve fit gives the dissociation constant of (68.3 ± 18.9) μM. The maximal shift is (11.6 ± 0.9) mV. Error bars show mean ± SD. The number of data points used for obtaining the mean values is shown in parentheses in the plots. The holding potential is −75 mV.

and Materials). The zero-current potential was −19 ± 3 mV (n = 10) and the membrane resistance was 580 ± 206 MΩ (n = 12) between −90 mV and 10 mV. Changes in these quantities by CPZ and TNP did not exceed the mean ± SD of each experiment.

Reduced turgor pressure and internal digestion

If the voltage shift as observed above was due to increased turgor pressure, the shift should be reduced or eliminated by applying suction at the recording pipette and reducing the initial cell volume. However, the voltage shift was almost

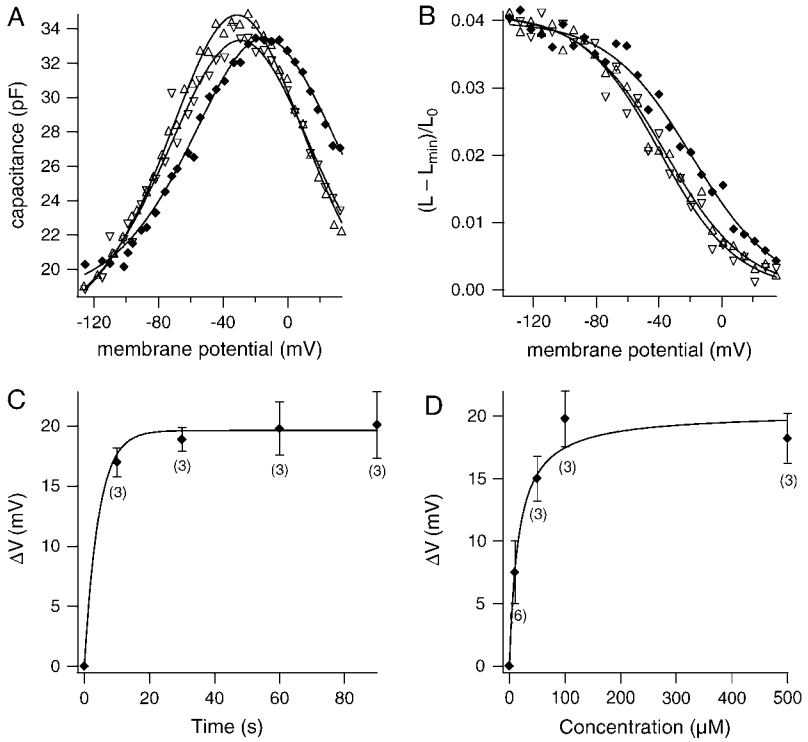

FIGURE 2 Effect of CPZ on voltage-dependent capacitance. (*A*) Effect on the membrane capacitance. Control (△), 50 μM CPZ (♦), and washout (▽). Parameter values for the curve fit. Control, q = (1.03 ± 0.02) e, C_{lin} = (17.1 ± 0.1) pF, and $V_{1/2}$ = (−37.5 ± 0.3) mV. 50 μM CPZ, q = (0.93 ± 0.01) e, C_{lin} = (17.7 ± 0.4) pF, and $V_{1/2}$ = (−25.2 ± 0.2) mV. Washout, q = (0.88 ± 0.04) e, C_{lin} = (16.2 ± 0.1) pF, and $V_{1/2}$ = (−33.6 ± 0.5) mV. (*B*) Length changes of the cell recorded during the capacitance measurement shown in panel *A*. Control (△), 50 μM CPZ (♦), and washout (▽). Parameter values for the fit. Control, q = (1.0 ± 0.11) e, $V_{1/2}$ = (−36.3 ± 2.6) mV, and $\Delta L_{max}/L_0$ = (0.041 ± 0.002). 100 μM CPZ, q = (0.98 ± 0.15) e, $V_{1/2}$ = (−19.2 ± 4.8) mV, and $\Delta L_{max}/L_0$ = (0.040 ± 0.004). Washout, q = (1.05 ± 0.15) e, $V_{1/2}$ = (−39.4 ± 3.3) mV, and $\Delta L_{max}/L_0$ = (0.041 ± 0.003). (*C*) Time course of voltage shift with 100 μM CPZ. The time constant is (4.3 ± 0.5) s. The saturating shift is (19.6 ± 0.6) mV. (*D*) Dose response of the voltage shift. The dissociation constant is ~(16.1 ± 3.7) μM. The maximal shift is (20.3 ± 1.2) mV. Error bars show mean ± SD. The number of data points used for obtaining the mean values is shown in parentheses in the plots. The holding potential is −75 mV.

TABLE 1 Changes in the characteristic parameters induced by membrane-bending chemicals

		Voltage dependence			Length change at V_h	
Chemical (property)	Conc. (μM)	$q_p - q_c$ (e)	$V_{1/2,p} - V_{1/2,c}$ (mV)	N	$(L_{0p} - L_{0c})/L_{0c}$ (%)	N
Procaine (cup-former)	500	-0.02 ± 0.06	11.2 ± 3.4	3	-6.2 ± 2.2	3
CPZ (cup-former)	50	-0.01 ± 0.12	13.7 ± 2.8	4	-4.8 ± 0.8	3
Dipyridamole (crenator)	200	-0.04 ± 0.08	14.1 ± 5.1	4	-6.1 ± 3.3	3
TNP (crenator)	500	-0.04 ± 0.11	11.5 ± 2.8	9	-7.5 ± 1.3	4

The holding potential V_h was -75 mV. The parameter values were determined by Eqs. 1–3. The changes listed (mean $\pm$ SD) were obtained from control values (subscript c), which were pooled pre-perfusion and washout data points, and values during perfusion (subscript p).

unchanged by such a manipulation (Fig. 4 *A*). The shift due to 500 μM TNP was (11.3 $\pm$ 2.3) mV ($n = 3$) and 100 μM CPZ induced a shift of (16.9 $\pm$ 1.2) mV ($n = 4$) (Fig. 4 *C*).

The effect of amphipathic ions could possibly be associated with their effect on the cortical cytoskeleton. To test this idea, some cells were injected from the patch pipette with the internal medium containing 0.1 mg/ml trypsin in the whole-cell configuration. Those cells turned into spheres (Fig. 4 *B*). Those cells did not recover their cylindrical shape by suction, demonstrating digestion of the cytoskeleton. These cells showed voltage shifts of (8.5 $\pm$ 1.2) mV ($n = 8$) with 500 μM TNP and (16.4 $\pm$ 1.1) mV ($n = 4$) with 100 μM CPZ (Fig. 4 *C*).

These observations indicated that pressure difference across the membrane, which increased membrane tension, was insignificant for the voltage shifts induced by CPZ and TNP. Instead, the shifts were likely associated with bending of the plasma membrane induced by these amphipathic ions. In the Discussion, we will show that a reduction of length does not need to result in a significant increase in tension using a theoretical model.

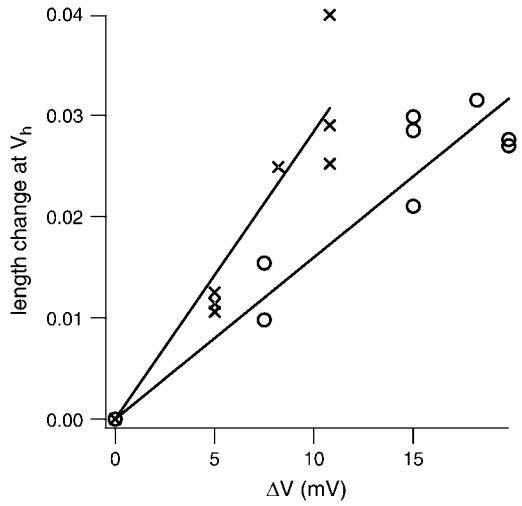

FIGURE 3 Correlation between length changes due to CPZ and TNP and voltage-shift ΔV induced by these chemicals. The slopes of the least-square fit are (0.28 $\pm$ 0.01) unit strain/mV for TNP-treated cells (X) and (0.16 $\pm$ 0.01) unit strain/mV for CPZ-treated cells (○). The holding potential is -75 mV.

DISCUSSION

On the perfusion with CPZ and TNP, NLC showed positive shifts, which are accompanied by reduced cell length at the holding potential. This observation could be explained by an increase in turgor pressure, which reduces the cell length and a positive shift in the voltage dependence of the NLC (8,24,25). However, these positive shifts of the NLC cannot be due to increased turgor pressure that results in increased membrane tension because these shifts were present even if the cells were deflated.

Length changes due to CPZ and TNP

Shouldn't a reduction in the length of cell body be accompanied by an increase in the turgor pressure of the cell, which leads to a positive shift of its NLC? To address this question, we examine a simple model for outer hair cells, assuming that the cell is approximated by an elastic cylinder. Following previous treatments, we additionally assume orthotropic elasticity of the outer hair cell membrane, which is characterized by two diagonal elastic moduli d_1 and d_2 and a cross modulus c (13,20).

Consider a cylinder of length L and radius R under stress-free condition. Pressure P applied to the interior of the cell would displace the cell membrane and change the length and radius of the cell to L' and R', respectively. If the elastic strain in the axial direction ϵ_{ze} ($= (L' - L)/L$) and that in the circumferential direction ϵ_{re} ($= (R' - R)/R$) are small, the constitutive equations can be expressed using the radius R before displacements (13,20),

$$\begin{bmatrix} d_1 & c \\ c & d_2 \end{bmatrix} \begin{bmatrix} \epsilon_{ze} \\ \epsilon_{re} \end{bmatrix} = \begin{bmatrix} 1/2 \\ 1 \end{bmatrix} RP. \quad (4)$$

The left-hand side is tension associated with elastic strains. The right-hand side is membrane tension due to pressure difference P across the membrane. The axial component T_z ($= RP/2$) is obtained by dividing the axial force $\pi R^2 P$ by the circumference $2\pi R$. The circumferential tension T_r ($= RP$) is obtained by dividing force $2RL$ tangential to the membrane by the length $2L$ of the membrane to which the force is applied. Membrane tension is thus anisotropic, the circumferential component being twice of the axial component.

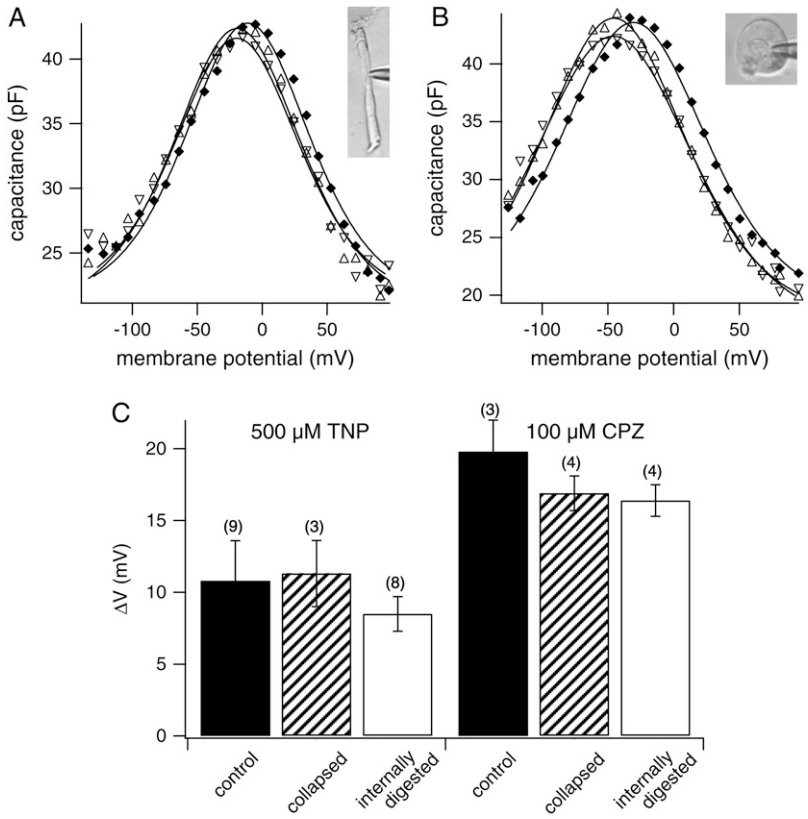

FIGURE 4 Effects of reduced turgor pressure and of internal digestion on voltage shifts induced by CPZ and TNP. (*A*) Effect of 500 μM TNP on the membrane capacitance in turgor pressure-reduced OHCs. Turgor pressure is reduced by applying negative pressure through recording pipette. Control (△), 500 μM TNP (♦), and washout (▽). Parameter values for the curve fit. Control, $q = (0.79 \pm 0.05)\ e$, $C_{lin} = (20.6 \pm 0.1)$ pF, and $V_{1/2} = (-19.2 \pm 1.2)$ mV. 500 μM TNP, $q = (0.81 \pm 0.05)\ e$, $C_{lin} = (21.2 \pm 0.1)$ pF, and $V_{1/2} = (-11.4 \pm 1.2)$ mV. Washout, $q = (0.80 \pm 0.06)\ e$, $C_{lin} = (21.2 \pm 0.1)$ pF, and $V_{1/2} = (-19.7 \pm 1.3)$ mV. (*B*) Effects of CPZ on a trypsin-treated outer hair cell. The intracellular medium with 0.1 mg/ml trypsin is injected to the cell from the patch pipette. The cell is not fully inflated. Control (△), 100 μM CPZ (♦), and washout (▽). Parameter values for the curve fit. Control, $q = (0.98 \pm 0.02)\ e$, $C_{lin} = (16.4 \pm 0.1)$ pF, and $V_{1/2} = (-18.7 \pm 1.1)$ mV. 100 μM CPZ, $q = (0.91 \pm 0.03)\ e$, $C_{lin} = (18.6 \pm 0.1)$ pF, and $V_{1/2} = (-1.8 \pm 1.1)$ mV. Washout, $q = (0.94 \pm 0.02)\ e$, $C_{lin} = (16.1 \pm 0.2)$ pF, and $V_{1/2} = (-13.0 \pm 1.7)$ mV. The holding potential is -75 mV. (*C*) Comparison of voltage shifts due to 500 μM TNP and 100 μM CPZ. Error bars show mean ± SD. The holding potential is -75 mV.

Now we assume that the total strains ϵ_z and ϵ_r are all elastic. That is, $\epsilon_z = \epsilon_{ze}$ and $\epsilon_r = \epsilon_{re}$. This situation corresponds to either direct application of pressure by the patch pipette in the whole-cell recording configuration or hyposmotic perfusion. Equation 4 leads to a stress-strain relationship,

$$T_z^{osm} = -\frac{d_1 d_2 - c^2}{2c - d_2}\epsilon_z. \tag{5}$$

Note here that Eq. 5 represents the cell deformation due to a pressure change and it is associated in the volume strain ϵ_v, which can be expressed by $\epsilon_z + 2\epsilon_r$ for the cylindrical geometry because the cell volume is proportional to LR^2,

$$\epsilon_v = \frac{4c - 4d_1 - d_2}{2(c^2 - d_1 d_2)}RP. \tag{6}$$

As expected, the volume strain E_v is proportional to pressure P.

Now we consider another type of cell deformation that does not change the volume strain. If microscopic bending of the membrane results in macroscopic displacement (see Fig. 5) but not in the elastic moduli, the total strains (ϵ_z, ϵ_r) can be expressed by the sum of elastic strains (ϵ_{ze}, ϵ_{re}) and strains (ϵ_{mb}, $\gamma\epsilon_{mb}$) induced by microscopic bending, where γ is a parameter. That is,

$$\begin{bmatrix}\epsilon_{ze}\\ \epsilon_{re}\end{bmatrix} = \begin{bmatrix}\epsilon_z\\ \epsilon_r\end{bmatrix} - \begin{bmatrix}\epsilon_{mb}\\ \gamma\epsilon_{mb}\end{bmatrix}. \tag{7}$$

The constant volume condition is represented by $\epsilon_z + 2\epsilon_r = \epsilon_{v0}$, where ϵ_{v0} is the volume strain and is a constant. By eliminating ϵ_r and ϵ_{mb} from these equations, we can obtain the axial tension T_z as a function of axial strain ϵ_z. Because tension increase T_z^{mb} induced by microscopic bending can be represented by $T_z(z) - T_z(0)$, we obtain

$$T_z^{mb} = \frac{\epsilon_z}{2}\frac{(c^2 - d_1 d_2)(2\gamma + 1)}{2d_1 - \gamma d_2 + c(2\gamma - 1)}. \tag{8}$$

This tension increase is associated with an increase in the pressure difference P across the membrane because $T_z = RP/2$.

For the same axial displacement, the ratio of tension increase due to microscopic bending to tension increase due to osmotic pressure is then given by

$$\frac{T_z^{mb}}{T_z^{osm}} = \frac{1}{2}\frac{(2\gamma + 1)(2c - d_2)}{2d_1 - \gamma d_2 + c(2\gamma - 1)}. \tag{9}$$

To illustrate the property of Eq. 9, we use the values for the elastic moduli $\{d_1, d_2, c\} = \{0.046, 0.068, 0.046\}$ N/m, which were determined from experimental data (13,20) and plot the ratio against the parameter γ (Fig. 6). The ratio of tension in the circumferential tension is the same because $T_r = 2T_z$ holds in both cases. It is also the ratio of pressure elevation. Since shifts in the voltage dependence of the motor are proportional to tension (8,13), we can use this ratio to evaluate expected voltage shifts.

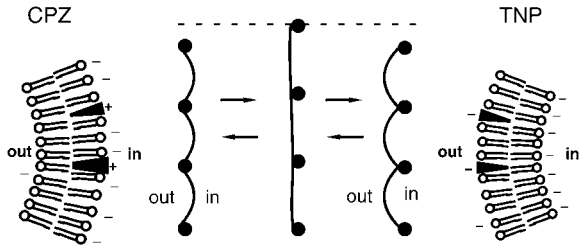

FIGURE 5 Schematic diagram showing that membrane bending can lead to shorting of the outer hair cells. Because the inner leaf of the plasma membrane is more negatively charged, positively charged CPZ is preferentially inserted into the inner leaf and negatively charged TNP is inserted into the outer leaf, bending the membrane in opposite directions. The lateral membrane of outer hair cells is stiffer in the circumferential direction than in the axial direction ($d_2 > d_1$). This anisotropy is thought to be based on stiff actin filaments, which run approximately in the circumferential direction. In the diagram, solid dots represent pillars and associated actin filaments that run in the perpendicular direction. Because of this mechanical anisotropy, reduction of apparent length takes place in the axial direction of the cell.

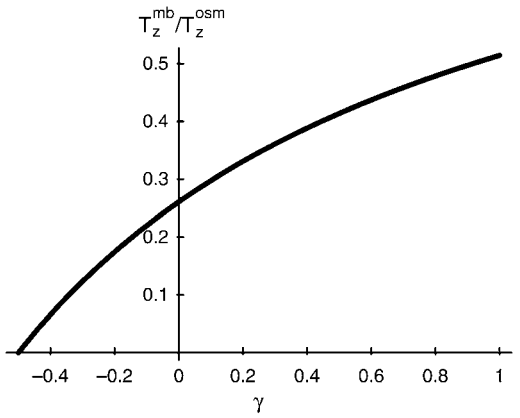

FIGURE 6 Dependence of membrane tension on the deformation anisotropy factor γ. Equation 9 is plotted against γ using experimentally determined values for elastic moduli d_1, d_2, $c = 0.046$, 0.068, and 0.046 N/m. If shrinkage of the apparent membrane area takes place as illustrated in Fig. 5, then $\gamma = 0$ and the development of tension due to deformation is one-quarter of osmotically induced tension increase.

The voltage shift due to osmotic stress is (144 ± 12) mV per unit strain (26). Thus, an osmotic stress associated with a 5% contraction of the cell length induces a 7.6 mV positive shift. There are two interesting cases for the values for γ. If the deformation is due to isotropic ($\gamma = 1$), the shift expected is 3.8 mV (=7.6 mV × 0.5). If microscopic bending has only the axial component ($\gamma = 0$) as illustrated in Fig. 5, the shift would be 1.9 mV (= 7.6 mV × 0.25), which is much smaller than the observed voltage shifts.

This result is not sensitive to a particular choice of elastic moduli. A set, $\{d_1, d_2, c\} = \{0.077, 0.077, 0.063\}$ N/m, which was obtained from cell displacements by applied pressure assuming isotropy (23), gives a value 0.27 for the tension ratio T_z^{mb}/T_z^{osm} at $\gamma = 0$, predicting a shift of 2.1 mV (= 7.6 mV × 0.27). Another set, $\{d_1, d_2, c\} = \{0.016, 0.056, 0.029\}$ N/m, which combines various data on the stiffness of outer hair cells (27), gives the value 0.33 for the tension ratio at $\gamma = 0$ and predicts a 2.5 mV shift.

This analysis shows that shortening of the cell due to microscopic bending of the plasma membrane does not raise pressure across the membrane enough to account for the observed voltage shifts. The voltage shifts observed must be a direct effect of microscopic bending of the membrane and not an indirect effect mediated by turgor pressure. Thus, the voltage shifts persist even if the cells become deflated.

A thermodynamic explanation

Why should the bending of the membrane in opposite directions shifts, the membrane motor's voltage dependence in the same positive direction? The free energy of the membrane motor may consist of terms that depend on membrane tension, hydrophobic mismatch at the lipid protein interface, and membrane torque (28–31). Since membrane tension should not be the major factor for the effect of the amphipathic ions we examined, we may need to consider hydrophobic mismatch and membrane torque.

Both CPZ and TNP could affect hydrophobic mismatch (28,29) and favor the extended state, leading to the voltage shift observed. However, if we assume that it is the reason for the voltage shifts, the close relationship between the cell length at −75 mV and shifts of the voltage dependence must be regarded as accidental. In addition, the linear capacitance should change (32) because the thickness of the membrane would be involved. However, we did not observe changes in the linear membrane capacitance that are associated with the perfusion of these amphipathic ions.

Membrane torque is associated with compression on one leaflet and extension on the other. CPZ and TNP should have opposite torque because of the difference in their electric charge. A free energy term that involves torque and splay of the membrane protein (28,30) depends on the direction of torque. This term depends on the direction of the torque and can account for the properties of TREK-1 and hTREK-1 channels that open with TNP and closes with CPZ (33,34). However, this term cannot explain our observation because the effect of CPZ is the opposite of that of TNP. A term in the free energy that does not depend on the direction of torque would be bending of the membrane protein.

Implications to motor models

What are the implications of our result on the mechanism of the membrane motor of outer hair cells? There are two major models for outer hair cell motility and the role of prestin, its major component (35).

One class of models is that the cellular motility of outer hair cells is based on a membrane motor, analogous to mechanosensitive channels in that it undergoes conformational

transitions that change their cross-sectional membrane area (8,10,12,13,36). A variation of this model is to consider a membrane machinery that produces mechanical stress (11). The number of conformational states of the motor could be more than two (36–38).

Based on a membrane motor model, our observations can be explained by assuming CPZ and TNP induce bending stress to the motor protein. It may be important that the amphipathic ions we tried only induce shifts in the voltage dependence of the motor and not the sensitivity. This result is consistent with two-state models because energy difference in the two states leads to only shifts of voltage dependence.

Our results may indicate some details on the two conformational states if we can estimate the curvature induced by CPZ and TNP and assume the membrane area of the motor. The voltage shift observed is up to 20 mV. The difference in the mechanical free energy in the two states must account for voltage shift of up to 20 mV that corresponds to 20 meV, or 3.2×10^{-21} J, because the charge involved is between 0.8 and 1 e.

How is the plasma membrane bent by CPZ and TNP? It could be reasonable to assume that the plasma membrane bends along the axial direction and that the nodes of membrane bending are at pillars that connect the plasma membrane with actin filaments (14). Thus the distance between the nodes is ~50 nm, reflecting the spacing between actin filaments (39). A reduction of length 5% due to bending corresponds to a membrane forming an arc of up to 1 radian. The corresponding radius of curvature R is 50 nm. If we further assume that the motor corresponds to the 10-nm particle (40,41), the bending energy E_{bb} of the bilayer that occupies the area of a motor can be expressed by

$$E_{bb} = \frac{1}{2} k_c \frac{A}{R^2}, \tag{10}$$

where A is the membrane area (42). The bending stiffness k_c of lipid bilayers is $1 - 10 \times 10^{-19}$ J (43). Thus, E_{bb} is $2 - 20 \times 10^{-21}$ J. The stiffness of membrane proteins would be larger than that of lipid bilayers. If we can use the formula of Landau and Lifshitz (44) for bending stiffness of solid plate YI, where Y is Young's modulus and I the moment, the bending stiffness is 2×10^{-18} J assuming the thickness of 5 nm and Young's modulus of 0.2 GPa (45). This value indicates that the bending stiffness of a membrane protein is likely greater than the lipid bilayer because the thickness of 5 nm is most likely an underestimate and the bending stiffness increases with the third power of thickness (44).

For these reasons, it is plausible that bending of the plasma membrane, in which the membrane motor is embedded, can be large enough to account for the voltage shift observed and that the extended state, which hyperpolarization favors, may be required to have a considerably lower bending stiffness than the other state.

The calculation given above is an order estimation. To build a theoretical model, one must consider microscopic bending of the lipid bilayer near the motor molecule to minimize hydrophobic mismatch, which is energetically costlier (46,47). This task is left for the future, because such a theory also needs to consider bending in the circumferential direction and requires detailed information on the motor molecule, such as the geometry.

What are the implications of our results on other models of electromotility? Particularly interesting is a model that posits that voltage-dependent membrane displacement is induced by changes of the membrane curvature (14–16). Let us call it a curvature-motor model for brevity. Amphipathic ions are expected to modulate the motor activity by increasing or decreasing the curvature of the plasma membrane (14).

This model has three problems in explaining our observations. First, the length of the cell at the holding potential. The curvature motor model assumes that cell length at the holding potential is determined by a non-zero natural curvature of the membrane. Bending of the membrane by CPZ and TNP should lead to changes in the cell length at a holding potential in the opposite direction. This prediction contradicts our observation that both CPZ and TNP shorten the cells.

Second, the shifts in the voltage dependence of electromotility. The curvature motor model predicts that CPZ and TNP, which bend the membrane in opposite directions, change the curvature from the natural curvature, shifting the operating point in opposite directions. Thus, it predicts opposite voltage shifts due to these ions. However, our experiment shows that both ions induce positive voltage shifts, contradicting the prediction of the curvature motor model.

Third, the voltage sensitivity of electromotility. Shifts in the operating point should also lead to changes in the voltage sensitivity. Thus, the curvature motor model predicts changes in voltage sensitivity of electromotility due to CPZ and TNP. However, we have observed only shifts and no significant changes in the steepness of the voltage dependence, contradicting the prediction. That was also the case for procaine and dipyrimidamole, additional membrane-bending agents that we examined. The implication of our results differ from that of previous reports (48,49), which compared the effects of CPZ and salicylate, another anionic amphipath. Since salicylate diminishes the voltage dependence (50,51) and CPZ does not, this contrast appeared consistent with the curvature motor model. However, salicylate appears to have specific interaction with prestin, the essential protein for the motor, because salicylate competes with Cl^- for a binding site that is critical for the activity of prestin (52).

CONCLUSIONS

Chlorpromazine (CPZ) and trinitrophenol (TNP), which bend the plasma membrane in opposite directions, act similarly in shifting the voltage-dependence of the outer hair cell (OHC) motor in the positive direction and in reducing the cell length at the holding potential. These effects are not associated with pressure buildup. They can be understood as

the result of microscopic bending of the plasma membrane by the amphipathic ions.

These observations are hard to explain based on the models that assume that electromotility is associated with curvature changes; they are consistent with the interpretation that the natural curvature of the outer hair cell membrane is not significant and that membrane motor is sensitive to membrane bending.

These results could be important for constraining molecular models for the membrane motor of outer hair cells because the membrane area and the thickness are significant for the bending stiffness. This issue is also related to the question as to what is the functional unit of prestin as a membrane motor, given that oligomerization of prestin has been reported (53,54).

We thank Dr. Richard Chadwick and Dr. Emilios Dimitriadis of National Institutes of Health, Dr. Joseph Santos-Sacchi of Yale University, and anonymous reviewers for useful comments.

This work is supported by the Intramural Research Program of National Institute on Deafness and Other Communication Disorders, National Institutes of Health.

REFERENCES

1. Brownell, W., C. Bader, D. Bertrand, and Y. Ribaupierre. 1985. Evoked mechanical responses of isolated outer hair cells. *Science*. 227:194–196.
2. Kachar, B., W. E. Brownell, R. Altschuler, and J. Fex. 1986. Electrokinetic shape changes of cochlear outer hair cells. *Nature*. 322:365–368.
3. Ashmore, J. F. 1987. A fast motile response in guinea-pig outer hair cells: the molecular basis of the cochlear amplifier. *J. Physiol.* (*Lond.*). 388:323–347.
4. Liberman, M. C., J. Gao, D. Z. He, X. Wu, S. Jia, and J. Zuo. 2002. Prestin is required for electromotility of the outer hair cell and for the cochlear amplifier. *Nature*. 419:300–304.
5. Zheng, J., W. Shen, D. Z.-Z. He, K. B. Long, L. D. Madison, and P. Dallos. 2000. Prestin is the motor protein of cochlear outer hair cells. *Nature*. 405:149–155.
6. Ashmore, J. F. 1990. Forward and reverse transduction in guinea-pig outer hair cells: the cellular basis of the cochlear amplifier. *Neurosci. Res. Suppl.* 12:S39–S50.
7. Santos-Sacchi, J. 1991. Reversible inhibition of voltage-dependent outer hair cell motility and capacitance. *J. Neurophysiol.* 11:3096–3110.
8. Iwasa, K. H. 1993. Effect of stress on the membrane capacitance of the auditory outer hair cell. *Biophys. J.* 65:492–498.
9. Dong, X. X., M. Ospeck, and K. H. Iwasa. 2002. Piezoelectric reciprocal relationship of the membrane motor in the cochlear outer hair cell. *Biophys. J.* 82:1254–1259.
10. Santos-Sacchi, J. 1993. Harmonics of outer hair cell motility. *Biophys. J.* 35:2217–2227.
11. Dallos, P., R. Hallworth, and B. N. Evans. 1993. Theory of electrically driven shape changes of cochlear outer hair cells. *J. Neurophysiol.* 70:299–323.
12. Ashmore, J. F. 1994. The cellular machinery of the cochlea. *Exp. Physiol.* 79:113–134.
13. Iwasa, K. H. 2001. A two-state piezoelectric model for outer hair cell motility. *Biophys. J.* 81:2495–2506.
14. Oghalai, J. S., H. B. Zhao, J. W. Kutz, and W. E. Brownell. 2000. Voltage- and tension-dependent lipid mobility in the outer hair cell plasma membrane. *Science*. 287:658–661.
15. Raphael, R. M., A. S. Popel, and W. E. Brownell. 2000. A membrane bending model of outer hair cell electromotility. *Biophys. J.* 78:2844–2862.
16. Zhang, P. C., A. M. Keleshian, and F. Sachs. 2001. Voltage-induced membrane movement. *Nature*. 413:428–432.
17. Sheetz, M. P., and S. J. Singer. 1976. Equilibrium and kinetic effects of drugs on the shapes of human erythrocytes. *J. Cell Biol.* 70:193–203.
18. Martinac, B., J. Adler, and C. Kung. 1990. Mechanosensitive ion channels of *E. coli* activated by amphipaths. *Nature*. 348:261–263.
19. Adachi, M., and K. H. Iwasa. 1999. Electrically driven motor in the outer hair cell: effect of a mechanical constraint. *Proc. Natl. Acad. Sci. USA*. 96:7244–7249.
20. Iwasa, K. H., and M. Adachi. 1997. Force generation in the outer hair cell of the cochlea. *Biophys. J.* 73:546–555.
21. Binford, J. S., and I. Wadso. 1984. Calorimetric determination of the partition coefficient for chlorpromazine hydrochloride in aqueous suspensions of dimyristoylphosphatidylcholine vesicles. *J. Biochem. Biophys. Methods*. 9:121–131.
22. Luxnat, M., and H. J. Galla. 1986. Partition of chlorpromazine into lipid bilayer membranes: the effect of membrane structure and composition. *Biochim. Biophys. Acta*. 856:274–282.
23. Iwasa, K. H., and R. S. Chadwick. 1992. Elasticity and active force generation of cochlear outer hair cells. *J. Acoust. Soc. Am.* 92:3169–3173.
24. Gale, J. E., and J. F. Ashmore. 1994. Charge displacement induced by rapid stretch in the basolateral membrane of the guinea-pig outer hair cell. *Proc. Roy. Soc. (Lond.) B Biol. Sci.* 255:233–249.
25. Kakehata, S., and J. Santos-Sacchi. 1995. Membrane tension directly shifts voltage dependence of outer hair cell motility and associated gating charge. *Biophys. J.* 68:2190–2197.
26. Adachi, M., M. Sugawara, and K. H. Iwasa. 2000. Effect of turgor pressure on outer hair cell motility. *J. Acoust. Soc. Am.* 108:2299–2306.
27. Tolomeo, J. A., and C. R. Steele. 1995. Orthotropic piezoelectric properties of the cochlear outer hair cell wall. *J. Acoust. Soc. Am.* 97:3006–3011.
28. Markin, V. S., and F. Sachs. 2004. Thermodynamics of mechanosensitivity. *Phys. Biol.* 1:110–124.
29. Lee, A. G. 2003. Lipid-protein interactions in biological membranes: a structural perspective. *Biochim. Biophys. Acta*. 1612:1–40.
30. Petrov, A. G., and P. N. Usherwood. 1994. Mechanosensitivity of cell membranes. ion channels, lipid matrix and cytoskeleton. *Eur. Biophys. J.* 23:1–19.
31. Perozo, E., A. Kloda, D. M. Cortes, and B. Martinac. 2002. Physical principles underlying the transduction of bilayer deformation forces during mechanosensitive channel gating. *Nat. Struct. Biol.* 9:696–703.
32. Awayda, M. S., W. Shao, F. Guo, M. Zeidel, and W. G. Hill. 2004. Enac-membrane interactions: regulation of channel activity by membrane order. *J. Gen. Physiol.* 123:709–727.
33. Patel, A. J., E. Honoré, F. Maingret, F. Lesage, M. Fink, F. Duprat, and M. Lazdunski. 1998. A mammalian two pore domain mechano-gated S-like K^+ channel. *EMBO J.* 17:4283–4290.
34. Miller, P., P. J. Kemp, A. Lewis, C. G. Chapman, H. J. Meadows, and C. Peers. 2003. Acute hypoxia occludes hTREK-1 modulation: re-evaluation of the potential role of tandem P domain K^+ channels in central neuroprotection. *J. Physiol.* (*Lond.*). 548:31–37.
35. Dallos, P., and B. Fakler. 2002. Prestin, a new type of motor protein. *Nat. Rev. Mol. Cell Biol.* 3:104–111.
36. Muallem, D., and J. F. Ashmore. 2006. An anion antiporter model of prestin, the outer hair cell motor protein. *Biophys. J.* 90:4035–4045.
37. Iwasa, K. H. 1997. Current noise spectrum and capacitance due to the membrane motor of the outer hair cell: theory. *Biophys. J.* 73:2965–2971.
38. Scherer, M. P., and A. W. Gummer. 2005. How many states can the motor molecule, prestin, assume in an electric field? *Biophys. J.* 88:L27–L29.

39. Holley, M. C., F. Kalinec, and B. Kachar. 1992. Structure of the cortical cytoskeleton in mammalian outer hair cells. *J. Cell Sci.* 102: 569–580.

40. Forge, A. 1991. Structural features of the lateral walls in mammalian cochlear outer hair cells. *Cell Tissue Res.* 265:473–483.

41. Kalinec, F., M. Holley, K. H. Iwasa, D. J. Lim, and B. Kachar. 1992. A membrane-based force generation mechanism in auditory sensory cells. *Proc. Natl. Acad. Sci. USA.* 89:8671–8675.

42. Helfrich, W. 1973. Elastic properties of lipid bilayers: theory and possible experiments. *Z. Naturforsch.* [*C*]. 28:693–703.

43. Waugh, R. E., J. Song, S. Svetina, and B. Zeks. 1992. Local and non-local curvature elasticity in bilayer membranes by tether formation from lecithin vesicles. *Biophys. J.* 61:974–982.

44. Landau, L. D., and E. M. Lifshitz. 1986. Theory of elasticity. *In* Course of Theoretical Physics, Vol. 7, 3rd Ed. Pergamon Press, Oxford, UK.

45. Zenchenko, T. A., E. V. Pozharskii, and V. N. Morozov. 1996. A magnetic micromethod to measure Young's modulus of protein crystals and other polymer materials. *J. Biochem. Biophys. Methods.* 33:207–215.

46. Cantor, R. S. 1997. The lateral pressure profile in membranes: a physical mechanism of general anesthesia. *Biochemistry.* 36:2339–2344.

47. Gullingsrud, J., and K. Schulten. 2004. Lipid bilayer pressure profiles and mechanosensitive channel gating. *Biophys. J.* 86:3496–3509.

48. Lue, A. J.-C., H.-B. Zhao, and W. E. Brownell. 2001. Chlorpromazine alters outer hair cell electromotility. *Otolaryngol. Head Neck Surg.* 125:71–76.

49. Morimoto, N., R. M. Raphael, A. Nygren, and W. E. Brownell. 2002. Excess plasma membrane and effects of ionic amphipaths on mechanics of outer hair cell lateral wall. *Am. J. Physiol. Cell Physiol.* 282:C1076–C1086.

50. Tunstall, M. J., J. E. Gale, and J. F. Ashmore. 1995. Action of salicylate on membrane capacitance of outer hair cells from the guinea-pig cochlea. *J. Physiol.* (*Lond.*). 485:739–752.

51. Kakehata, S., and J. Santos-Sacchi. 1996. Effects of salicylate and lanthanides on outer hair cell motility and associated gating charge. *J. Neurosci.* 16:4881–4889.

52. Oliver, D., D. Z. He, N. Klocker, J. Ludwig, U. Schulte, S. Waldegger, J. P. Ruppersberg, P. Dallos, and B. Fakler. 2001. Intracellular anions as the voltage sensor of prestin, the outer hair cell motor protein. *Science.* 292:2340–2343.

53. Navaratnam, D., J.-P. Bai, H. Samaranayake, and J. Santos-Sacchi. 2005. N-terminal-mediated homomultimerization of prestin, the outer hair cell motor protein. *Biophys. J.* 89:3345–3352.

54. Zheng, J., G.-G. Du, C. T. Anderson, J. P. Keller, A. Orem, P. Dallos, and M. Cheatham. 2006. Analysis of the oligomeric structure of the motor protein prestin. *J. Biol. Chem.* 281:19916–19924.